# Application of Alginate in Water Treatment and Drug Delivery Systems

Flinders
UNIVERSITY

A thesis submitted to the School of Chemical & Physical Sciences, Faculty of Science & Engineering, at Flinders University of South Australia in fulfilment of the degree of Doctor of Philosophy

September 2014

**Wafa Algothmi**

Supervisors: Professor Amanda V. Ellis,

Co-supervisors: Professor Joseph G. Shapter

# Table of Contents

# Declaration

I certify that this thesis does not incorporate without acknowledgment any material previously submitted for a degree or diploma in any university; and that to the best of my knowledge and belief it does not contain any material previously published or written by another person except where due reference is made in the text.

_____

Wafa Algothmi on _____/_____/_____

# Acknowledgements

First and foremost, praises and thanks to the God, the Almighty, for giving me the power of patience throughout my research work to complete the research successfully.

I would like to express my deep and sincere gratitude to my primary supervisor, Prof Amanda Ellis for her guidance, encouragement and patience throughout the years. I extremely grateful for her taking time to editing my thesis. Her sincerity and motivation have deeply inspired me. She has taught me the methodology to carry out the research and how to present the research clearly. It has been a great privilege to study and work under her guidance. I am extremely appreciative of what she has offered me.

I am extending my gratitude to my co-supervisor, Prof. Joe Shapter for taking time in editing my thesis. I would also like to thank members of the ever-changing Ellis research group, staff and academia at Flinders University for their help and kindness.

My special thanks to my husband for his patience, support, help and encouragement. I would like to thank my sons and daughter for being such quiet kids and always helping me. Many thanks to my parents for their love, caring and sacrifices for educating and preparing me for my future. Also, I express my thanks to my sisters and brothers for their support.

Finally, i would like to thank my funding source, Taif University, Saudi Arabia, for giving me the opportunity to complete my PhD degree.

# Abstract

This thesis covers both the use of Ca-$Alg_2$ hydrogels in water treatment and drug delivery system. Ca-$Alg_2$ and Ca-$Alg_2$/GO gel bead adsorbents fabricated for the removal of $Cu^{2+}$ ions from aqueous solution. The influence of the use of different adsorbent doses, $Cu^{2+}$ concentrations and contact time on the adsorption process was demonstrated that the larger surface area of GO and oxygen containing functional groups on the GO surface plays a strong role in increasing the adsorption capacity of Ca-$Alg_2$.

Chapter two discusses the loading of RB, Rubpy and CPT into Ca-$Alg_2$ hydrogel using the *in situ* addition method. The influence of the pH of the released medium affected on the release of both of dye and drug from Ca-$Alg_2$ hydrogel. The molecular weight and the charge of the dye or drug play an important role in the releas process from Ca-$Alg_2$ hydrogel. Furthermore, the release kinetic studies for both of dye and drug revealed that the release mechanisms of the three molecules at pH ~ 2.4 occurred via Fickian diffusion and Case II transport. However, at pH ~ 7.4, the release mechanisms was an anomalous transport.

This thesis also focused on synthesis and characterisation of β-CD-g-Alg. The characterisation of the CPT inclusion complexes (CPT/β-CD and CPT/β-CD-g-Alg) confirmed that the inclusion complexes were produced, and the results indicated that the amino quinoline group for CPT molecule is included into the β-CD cavity. Furthermore, the thermal analysis shows that the ratio of Na-Alg to β-CD appears to

be 2:1. The last section details the release profile of CPT from both inclusion complexes using the dialysis technique, and Fick's second law was used to analyse the release data. It was found that β-CD prolonged the release of CPT with initial burst release and reached the equilibrium after 9 days. However, the release of CPT from the CPT/β-CD-g-Alg inclusion complex did not show the initial burst release and the equilibrium was reached after 13 days. This result indicates that Na-Alg increased the solubility of CPT/β-CD inclusion complex and enhanced the formation of CPT/β-CD.

# Publications

Algothmi, W. M., Bandaru, N. M., Yu, Y., Shapter, J. G., & Ellis, A. V. "Alginate–graphene oxide hybrid gel beads: An efficient copper adsorbent material." *Journal of colloid and interface science* 397 (2013): 32-38.

.

# List of Figures

# List of tables

# Lists of abbreviations, symbols and units

| Symbol/acronym/unit | Translation/explanation |
|---|---|
| **Na-Alg** | Sodium alginate |
| **H-Alg** | Alginic acid |
| **G** | Guluronic |
| **GDL** | D-glucono-δ-lactone |
| **M** | Mannuronic |
| **$Ca^{2+}$** | Calcium (II) ions |
| **$Sr^{2+}$** | Strontium (II) ions |
| **$Ba^{2+}$** | Barium (II) ions |
| **pH** | Power of Hydrogen (per Hydrogen) |
| **$pK_a$** | Acidic constant |
| **$Cu^{2+}$** | Copper (II) ions |
| **$Ni^{2+}$** | Nickel (II) ions |
| **$Co^{2+}$** | Cobalt (II) ions |
| **$CaCO_3$** | Calcium carbonate |
| **$Na^{+}$** | Sodium (I) ions |
| **CNTs** | Carbon nanotubes |
| **GO** | Graphene oxide |
| **Å** | Angstrom |
| **DMF** | *N*,*N*-dimethylformamide |

| | |
|---|---|
| **NMP** | *N*-methylpyrrolidone |
| **THF** | Tetrahydrofuran |
| **$Zn^{2+}$** | Zinc (II) ions |
| **GO-MPs** | GO functionalised magnetic particles |
| **CS/GO** | Chitosan/graphene oxide |
| **$Au^{3+}$** | Gold (III) ions |
| **$Pd^{2+}$** | Lead (II) ions |
| **MC/GO** | Magnetic chitosan/graphene oxide |
| $q_{eq}$ | Adsorbed amount at equilibrium |
| $C_{eq}$ | Equilibrium concentration |
| **T** | Temperature |
| $V_L$ | Volume |
| **°C** | Degrees Celsius |
| $C_o$ | Initial concentration |
| $m_A$ | mass |
| $\Delta m^l$ | Mass removed from the liquid phase |
| $\Delta m^a$ | Mass adsorbed onto the adsorbent |
| $C$ | Mass concentration |
| $q$ | Adsorbent loading |
| **t** | Time |
| $q_m$ | Maximum adsorption capacity |

| | |
|---|---|
| ***b or $K_L$*** | Langmuir constant |
| **g $mol^{-1}$** | Grams per mole |
| **Ca-$Alg_2$** | Calcium alginate |
| **Ca-$Alg_2$/GO** | Calcium alginate/graphene oxide |
| **h** | Hour |
| **%** | Per cent |
| **CPT** | Camptothecin |
| **DTAB** | Dodecyltrimethylammonium bromide |
| **BSA** | Bovine serum albumin |
| **$CaCl_2$** | Calcium chloride |
| **Na-Alg/HPMC** | Sodium alginate/hydroxypropyl-methylcellulose |
| **Na-Alg-g-PCL** | Sodium alginate/poly(ε-caprolactone) |
| **NaCMC** | Sodium carboxymethyl cellulose |
| **MAS** | Magnesium aluminum silicate |
| **MPs** | Microspheres |
| **AAM-g-HES** | Acrylamide/hydroxyethyl cellulose |
| **CDs** | Cyclodextrins |
| **α-CD** | α-cyclodextrin |
| **β-CD** | β-cyclodextrin |
| **γ-CD** | γ-cyclodextrin |
| **$^1$H NMR** | $^1$H nuclear magnetic resonance |

| | |
|---|---|
| **FTIR** | Fourier transform infrared |
| **TGA** | Thermogravimetric analysis |
| **XRD** | X-ray diffraction |
| **DSC** | Differential scanning calorimetry |
| **DBA** | Dibenzalacetone |
| **CLA** | Crassicauline A |
| **HP-β-CD** | Hydroxypropyl-β-cyclodextrin |
| **RDM-β-CD** | Randomly substituted dimethyl-β-cyclodextrin |
| **RDM-γ-CD** | Randomly substituted dimethyl-γ-cyclodextrin |
| **M, mol $L^{-1}$** | Moles per litre |
| **β-CD-*graft*-PAsp** | β-cyclodextrin-grafted-α, β-poly (aspartic acid) |
| **nm** | Nanometer |
| **mL** | Millilitre |
| **wt/wt %** | Weight per weight per cent |
| **g** | Grams |
| **min** | Minute |
| **mM** | Millimolar |
| ***W*** | Weight |
| **L** | Litre |
| **mg $L^{-1}$** | Milligrams per litre |
| $C_e$ | Final concentration |

| | |
|---|---|
| $q_t$ | Adsorption capacity at time *t* |
| **mg g$^{-1}$** | Milligrams per gram |
| $C_t$ | Concentration at time *t* |
| **KBr** | Potassium bromide |
| **mL min$^{-1}$** | Millilitres per minute |
| **FIB/SEM** | Focused ion beam scanning electron microscopy |
| **cm** | Centimeters |
| **RB** | Rose Bengal |
| **Rubpy** | Tris(2,2'-bipyridyl) dichlororuthenium (II) hexahydrate |
| **DMSO** | Dimethylsulfoxide |
| **mm** | millimeter |
| **UV** | Ultra violet |
| **UV-vis** | Ultra violet-visible |
| **π** | Pi |
| **ATR-FTIR** | Attenuated total reflection-Fourier transform infrared spectroscopy |
| **β-CD-g-Alg** | β–cyclodextrin-grafted-alginate |
| **β-CD-6-OTs** | Mono-6-deoxy-6-(*p*-toluenesulfonyl ) β–cyclodextrin |
| **$Ts_2O$** | *ρ*-Toluenesulfonic anhydride |
| **$NH_4Cl$** | Ammonium chloride |
| **TBA-Alg** | Tetrabutylammonium-alginate |

| | |
|---|---|
| **N** | Normality |
| **TBAOH** | Tetrabutylammonium hydroxide |
| **v/v** | Volume per volume |
| **δ** | Chemical shifts |
| **ppm** | Parts per million |
| $K_2$ | Rate constant of pseudo-second-order adsorption |
| **C=O** | Carbonyl |
| **O-H** | Hydroxyl |
| $T_{max}$ | Maximum decomposition |
| $T_i$ | Initial temperature |
| $T_f$ | Final temperature |
| **µM** | Micrometer |
| **g** $L^{-1}$ | Gram per litre |
| **Chitosan-GLA** | Chitosan-glutaraldehyde |
| $R^2$ | Correlation coefficient |
| $T_g$ | Glass transition temperature |
| $R_{diff}$ | Diffusion rate |
| $R_{relax}$ | Relaxation rate |
| $M_t$ | Amounts of drug released at time *t* |
| $M_\infty$ | Amounts of drug released at infinite time |
| ***n*** | Release exponent |

| | |
|---|---|
| ***a*** | Scale parameter |
| ***b*** | Shape parameter |
| $\lambda_{max}$ | Lambda maximum (wavelength) |
| $H^+$ | Hydrogen ions |
| ***D*** | Diffusion coefficient |
| ***l*** | Thickness |
| ***s*** | Second |
| $-SO_2-O-$ | Sulfonate |
| $TBA^+$ | Tetrabutylammonium counterion |
| **COO-** | carboxyl group |
| $D_2O$ | Deuterium oxide |
| **d6-DMSO** | Deuterated dimethylsulphoxide |
| **CNBr** | Cyanogen bromide |
| **NR** | Neutral red |
| ***x*** | Distance |
| **Σ** | Summation |
| **HPMC** | Hydroxypropylmethylcellulose |
| **PVP** | Polyvinylpyrrolidone |
| **CMC** | Carboxymethylcellulose |
| **β-CD-dextrin** | β-cyclodextrin-dextran |
| **HC** | Hydrocortisone |

| | |
|---|---|
| **$D_1$** | Diffusion coefficient for the fast release |
| **$D_2$** | Diffusion coefficient for the slow release |
| **RF** | Riboflavin |
| **PLGA** | Poly(lactide-*co*-glycolide) |
| **PCL** | Poly-ε-caprolactone |
| **W/O/W** | Water in oil in water |
| **π** | π is the ratio of a circle's circumference to its diameter (π = 3.1415) |

# Thesis guide

## Objectives of the research

The main objectives of this thesis were to introduce methods for the preparation of an efficient material from sodium alginate for use as an adsorbent in water treatment and as a delivery vehicle in a drug delivery system. In order to achieve these objectives detailed descriptions of the milestones were as follows:

1- Calcium alginate (Ca-$Alg_2$) and calcium alginate with encapsulated graphene oxide (Ca-$Alg_2$/GO) gel bead adsorbents were fabricated. The ability of Ca-$Alg_2$ and Ca-$Alg_2$/GO gel beads to remove copper ions from aqueous solutions was investigated by varying the parameters; adsorbent doses, $Cu^{2+}$ concentrations and contact times. The kinetic studies of the adsorption process were investigated.

2- The Ca-$Alg_2$ hydrogel was loaded with three different molecules; rose Bengal (RB), Tris(2,2'-bipyridyl) dichlororuthenium (II) hexahydrate (Rubpy) and camptothecin (CPT). Release of the three molecules from Ca-$Alg_2$ hydrogel at different pH's were monitored using UV-vis or fluorescence spectroscopies. The release mechanisms of RB, Rubpy and CPT from the Ca-$Alg_2$ hydrogels were studied using Ritger-Peppas and Weibull models. The diffusion coefficients of RB, Rubpy and CPT were determined using the Ritger-Peppas model.

3- β-cyclodextrin grafted sodium alginate (β-CD-g-Alg) was prepared and characterised. Subsequently, CPT inclusion complexes with β-CD (CPT/ β-CD) and β-CD-g-Alg (CPT/ β-CD-g-Alg) were fabricated and characterised using the a variety of scientific techniques such as attenuated total reflection-Fourier transform infrared (ATR-FTIR) and proton nuclear magnetic resonance ($^1$H NMR) spectroscopies.

4- The ability of the CPT/ β-CD-g-Alg inclusion complex in retarding the release of CPT was investigated and compared with the release of free CPT and CPT from CPT/ β-CD inclusion complexes. The diffusion coefficient values were then determined using Fick's second law.

## Layout of thesis

This thesis consists of seven chapters wherein Chapter 1 describes the introduction of the polysaccharide polymer, sodium alginate and a literature review on Na-Alg as an adsorbent material in water treatment and as a delivery vehicle in drug delivery systems. The materials and the experimental procedures used throughout this thesis are described in Chapter 2. In this chapter, a brief description of the analytical instruments used throughout the studies is also given. Chapter 3 describes the preparation of Ca-$Alg_2$ and Ca-$Alg_2$/GO gel bead adsorbents, and their ability in the removal of $Cu^{2+}$ ions from aqueous solutions is investigated. The release profiles of RB, Rubpy and CPT from the Ca-$Alg_2$ hydrogels are demonstrated in Chapter 4. Here the release mechanisms of RB, Rubpy and CPT are explained and the diffusion coefficients calculated. In Chapter 5, β-CD-g-Alg, CPT/ β-CD and CPT/ β-CD-g-Alg inclusion complexes are synthesised and characterised. In Chapter 6 the release profiles and the diffusion coefficients of CPT from CPT/ β-CD and CPT/ β-CD-g-Alg inclusion complexes were investigated. Chapter 7 concludes the previous chapters.

# Chapter 1. Introduction and literature review

## 1.1 Synopsis

*Background information relevant to this thesis will be outlined in this chapter. The structure and the properties of sodium alginate (Na-Alg) will be discussed. This includes the formation and gelation mechanism. The properties of graphene oxide (GO) will be discussed. Particular attention will be drawn towards the potential of using Ca-Alg$_2$ and GO as adsorbents materials in water treatment as evident in the current literature. This is followed by a discussion on the drug delivery system and this includes literature review on the use of the hydrogel as a drug delivery system. The importance of beta-cyclodextrin (β -CD) for improved drug delivery systems will also be introduced, and it was chosen to modify Na-Alg in this research.*

## 1.2 Background on alginate

### 1.2.1 Structure of sodium alginate (Na-Alg)

Sodium alginate (Na-Alg), the sodium salt form of alginic acid (H-Alg), is a linear copolymer containing varying proportions of 1,4-linked β–D–mannuronic acid (M-blocks) (Figure 1.1a) and α–L guluronic acid (G-blocks) (Figure 1.1b) residues in a pyranose form [1]. These monomers are arranged as a series of block structures which may be homopolymer blocks (MM-blocks or GG-blocks) or copolymer blocks (MG- blocks) (Figure 1.1c) [1].

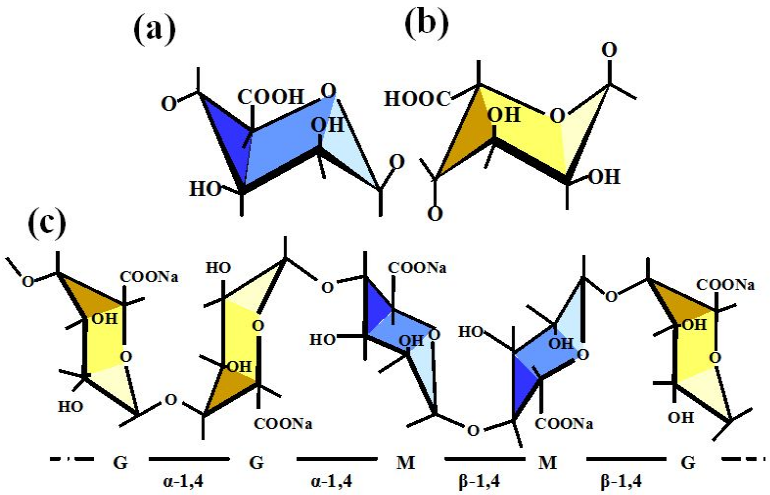


Figure 1-1 Alginate composition. (a) β-D-mannuronic acid, (b) α-L-guluronic acid and (c) various structural formulae of sodium alginate [1].

### 1.2.2 Production of Na-Alg

Na-Alg is often isolated from several types of brown algae [2]. Currently, it is predominately extracted from *Macrocystis sp., Laminaria sp.* and *Ascophyllum sp.,* which are the major genera of marine brown algae [2]. In addition, Na-Alg can be produced by two species of bacteria namely, *Azotobacter vinelandii* and *Pseudomonas aeruginosa* [3]. Figure 1.2 represents a schematic of the extraction process from brown algae, and contains the following steps [4]:

- Removal of the counter ions (sodium, calcium, magnesium, strontium and barium ions) via proton exchange using a mineral acid to produce water insoluble H-Alg.
- Neutralisation of H-Alg with an alkali (sodium carbonate or sodium hydroxide) to form water soluble (Na-Alg).
- Removal of particulate matter using a separation process such as sifting, flotation, centrifugation or filtration.
- Precipitation of the Na-Alg with alcohol, calcium chloride or a mineral acid, then drying and milling.

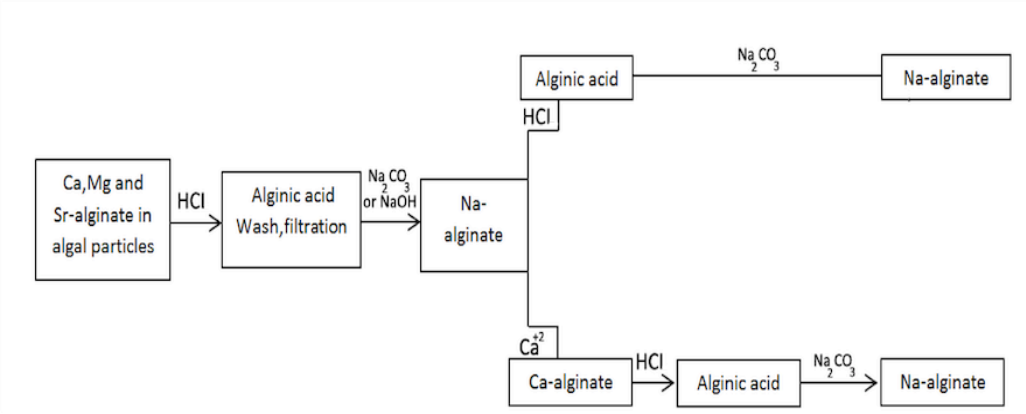


Figure 1-2 Schematic diagram of the typical extraction process of sodium alginate from brown algae [4].

### 1.2.3 Physical properties of Na-Alg

#### 1.2.3.1 Solubility

The solubility of alginates in water is dependent on the pH of the solvent, ionic strength of the solute and the content of gelling ions in the solvent [5]. Addition of gelling ions for example divalent metal ions to the solvent decreases the solubility of alginate due to gel-formation [6].

The pH of the solvent plays an important role in the solubility of alginate. It is essential that the carboxylic acid groups (Figure 1.1) be deprotonated to make alginate soluble [5]. In alginate, the mannuronic and guluronic acid monomers have $pK_a$ values of 3.38 and 3.65, respectively, making them negatively charged at near neutral pH and thus soluble [7]. However, any decrease in pH of the solvent below the $pK_a$ values of the two monomers causes insoluble alginate [5].

Na-Alg is the most common form of deprotonated H-Alg and is soluble in water but insoluble in most organic solvents, while H-Alg, with its carboxylic acid groups (in their protonated form), is insoluble in both water and organic solvents [4].

The solubility of alginate also depends on the chemical composition and sequence of the alginate structure [8]. For example, in acidic solution alginate that contains a copolymer structure (MG-blocks) will precipitate at a lower pH compared with alginate that contains a homopolymer structure (MM-blocks or GG-blocks). This has been observed with *Ascophyllum nodosum* alginate which has a copolymer structure [8]. Huag et al. [8] observed that alginate had a higher solubility in acidic solution due to its lower proportion of homopolymer blocks.

An additional consideration in alginate solubility is ionic strength of the alginate solution. It has been shown that any change in ionic strength has a significant effect on the alginate polymer chain extension, the viscosity of solution and the solubility in an alginate solution [9]. Haug [10] studied the solubility of alginate in potassium chloride solution of different strengths. It was found that the one third of the alginate

is soluble and two thirds insoluble in solution, which contain between 0.6 and 1 M potassium chloride [10]. Lastly, the presence of divalent cations such as $Ca^{2+}$, $Sr^{2+}$ and $Ba^{2+}$ has an effect on the solubility of alginate by acting as cross-linkers (or gelling agents) [6]. This important concept will be discussed further in the follow section.

## 1.2.4 Ionic cross-linking for gel formation

### 1.2.4.1 Types of cross-linking

Alginate can form a gel structure by replacement of, for example $Na^+$ ions by polyvalent metal ions, as shown in Equation 1.1 [11]. This ultimately leads to the formation of ionotropic metal alginate complexes [12].

$$Z\,(Na\text{-}Alg)_n \;+\; nM^{Z+} \;=\; (M\text{-}Alg_Z)_n \;+\; Z\,Na^+$$

*sol* *electrolyte* *complex* *electrolyte*

Equation 1.1

In these ionotropic gels, the metal ion chelates with the functional groups (carboxyl and hydroxyl groups) of the macromolecular chains of alginate [13]. This chelation depends on the chemical composition of alginate [14] and the cross-linked metal ions (coordination number and valency) [11, 13].

In particular, alginate that contains more mannuronic acid residues has a lower affinity to calcium ions in the sodium–calcium cation exchange cross-linking process. Whereas alginate that contains more guluronic residues [14] has a higher calcium ion affinity due to the spatial arrangement of the G-G block zone [15, 16] This arrangement of the cross-linked area is called an “Egg-box,” (see Figure 1.3) [15, 16].

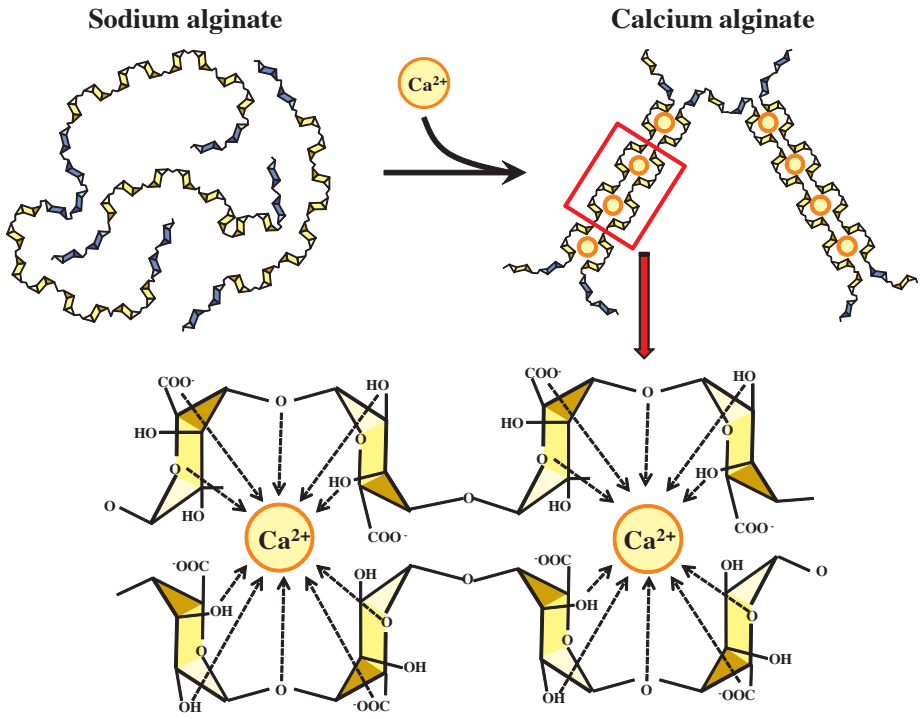


Figure 1-3 Binding of divalent cations by alginate (Egg-box) model [1].

In this model, two pairs of G-alginate chains create pocket-like cavities in which $Ca^{2+}$ cations can be located between them, called a junction zone [17, 18]. In this case a 4:1 ratio between G units and $Ca^{2+}$ cations exists [18]. $Ca^{2+}$ cations are separated by a distance of 0.86 nm along the chain axis, and the lateral interaction between dimers takes place through nonspecific interactions such as disordered $Na^{+}$ or $Ca^{2+}$ cations and water-mediated hydrogen bonding (see Figure 1.4(a)) [18]. The long-range order between dimers requires that the $Ca^{2+}$ cations be located at two defined crystallographic positions, which separated by a distance of $c/2$ = 0.43 nm (see Figure 1.4(b)) [18].

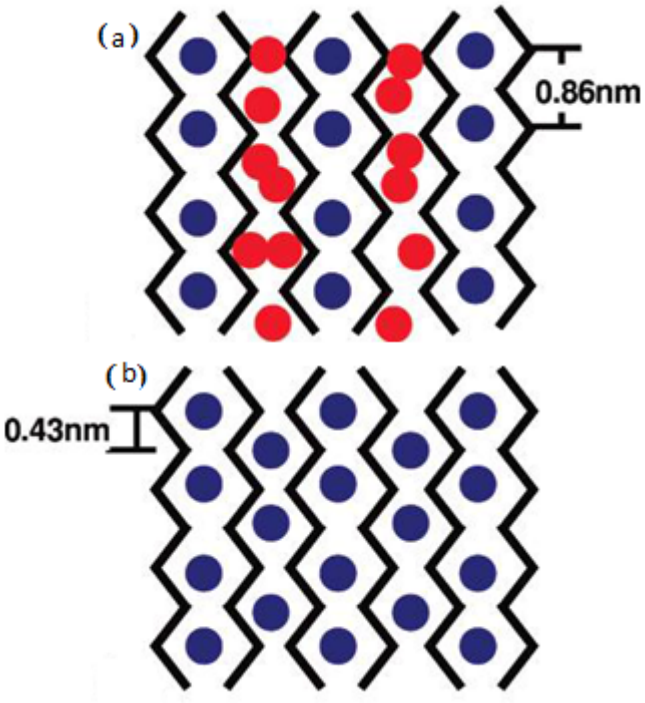


Figure 1-4 Schematic structure of G-alginate junction zone. (a) $Ca^{2+}$ (blue dots) located along the chain axis and $Na^{+}$ or $Ca^{2+}$ (red dots) located between alginate dimers that pack through unspecific interactions and (b) long-range $Ca^{2+}$ located between interacting chains [18].

The chelation between the metal ion and the functional groups in the ionotropic complex may be either intramolecular, in which the carboxyl and hydroxyl groups belong to the same chain, or intermolecular in which the functional groups belong to the different chains in order to attain a stable coordination geometry [19].

In the case of divalent metal ions (e.g., $Cu^{2+}$, $Ni^{2+}$ and $Co^{2+}$) the polyelectrolyte alginate anions are converted into ionotropic metal alginate complexes, such as copper alginate (Cu-$Alg_2$), nickel alginate (Ni-$Alg_2$) and cobalt alginate (Co-$Alg_2$) [12, 20, 21]. The geometrical structure of these types of complexes depends on the coordination number of the metal ion, thus divalent metal ions are chelated with two carboxyl groups and one or two pairs of the hydroxyl groups on the uronic acids [12, 20, 21]. Hence two geometrical structures (intramolecular and intermolecular) are possible in chelation (see Figure 1.5) [13].

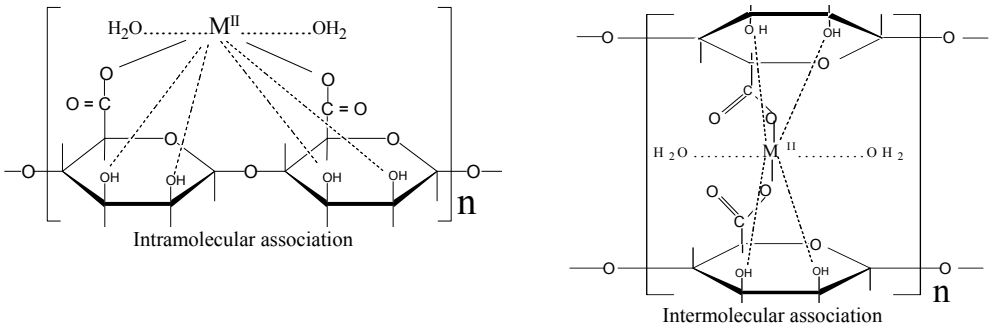


Figure 1-5 Intramolecular (left) and intermolecular (right) geometrical structures of divalent metal alginate ionotropic complexes [19].

On the other hand trivalent metal ions are chelated with three carboxyl groups and one or more pairs of hydroxyl groups in the uronic acid. This chelation, which depends on the coordination number of the metal ion, is restricted to only an intermolecular association mechanism in order to decrease the bond stretching resulting from the expansion of the metal-oxygen bond in the intramolecular association mechanism, as shown in Figure 1.6.

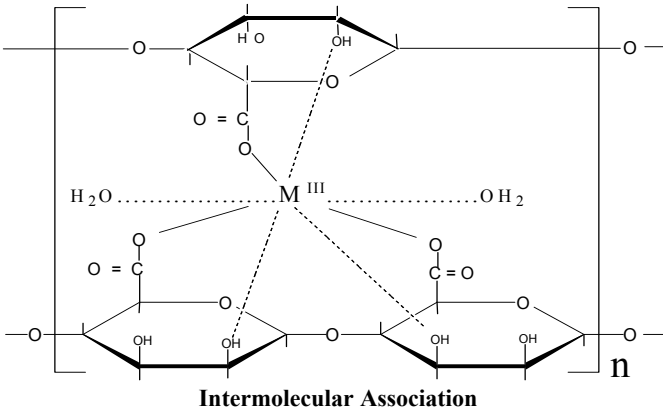


Figure 1-6 Intermolecular geometrical structure of a trivalent metal ionotropic alginate complex [11].

There are two fundamentally different methods of preparing an alginate gel: Using cations as cross-linking agents:

1. The diffusion method (or external method) wherein a cross-linking ion (e.g., $Ca^{2+}$) diffuses into the alginate solution from the metal ion solution, as shown in Figure 1.7(a) [22]. This method exhibits an inhomogeneous distribution of alginate and rapid gelling kinetics are used for cation immobilisation purposes [9].
2. The internal method (*in-situ* gelation) wherein a cross-linking cation (e.g., $Ca^{2+}$) is controlled released from an inert calcium solution (commonly $CaCO_3$) within the alginate solution to give homogeneous gels, as shown in Figure. 1.7(b) [23]

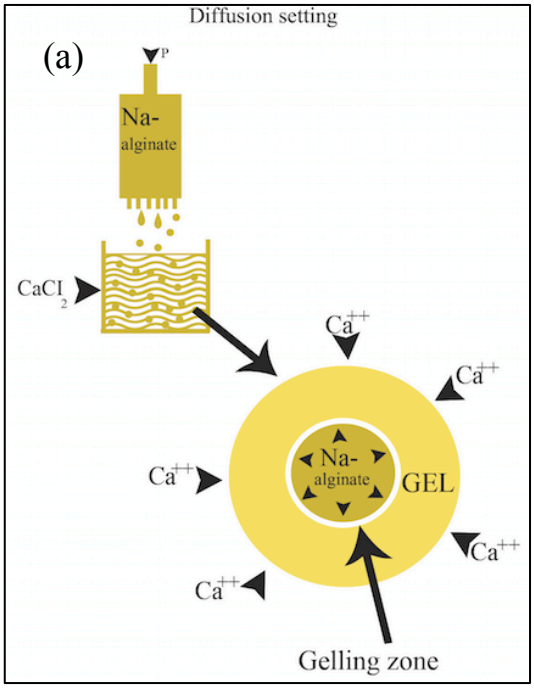


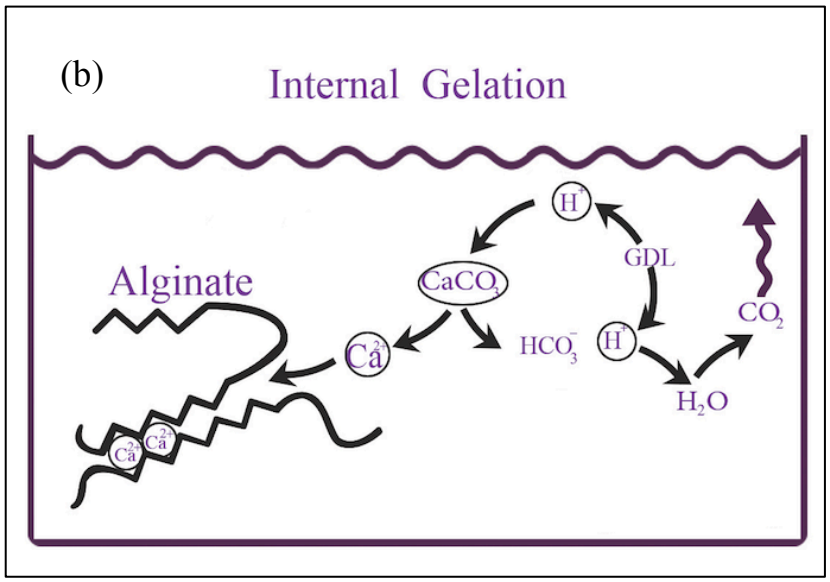


Figure 1-7 Depiction of two fundamental methods for preparing alginate gel. (a) the diffusion or external method and (b) the internal method [9].

The difference in gelation mechanisms between the external and internal methods results in different gel structures with different properties [24]. The diffusion (or external) method produces cross-linked gels with smooth surfaces, greater matrix strength, stiffness and permeability than the internal cross-linked matrix [24]. Furthermore, external cross-linking is capable of greater drug encapsulation efficiency and slower drug release rates [24].

The following section describes in more detail the gelation mechanism behind the use of the diffusion or external cross-linking method.

#### 1.2.4.2 Gelation mechanism of the diffusion (or external) cross-linking method

When an electrolyte solution of a polyvalent metal ion such as a $Ca^{2+}$ cation is carefully brought into contact with a sodium alginate polyanion sol the counterions of the electrolyte solution slowly diffuse into the alginate sol [25, 26]. The diffusing counterions are attracted to the oppositely charged sites on the polyelectrolyte molecules, thereby reducing the charge density of the latter and diminishing their tendency to hydrate [25, 26]. This leads to the formation of a thin primary membrane at the interface between the alginate sol and the metal ion electrolyte [25, 26]. This primary membrane prevents the colloidal polyelectrolyte from diffusing into the electrolyte sol [25, 26]. Hence, the macromolecular chains of the alginate sol start to distribute themselves below the already formed primary membrane [25, 26]. As a steady state is approached, the metal ions of the electrolyte begin to diffuse through the already formed membrane inside the alginate sol [25, 26]. Simultaneously, the counterions resulting from the dissociation of the sol, i.e., $Na^{+}$ ions, start to diffuse through the membrane into the electrolyte [25, 26].

Because diffusion or external method is the preferred method in producing cross-linked alginate for encapsulation purposes, this thesis utilises this method to produce cross-linked Ca-$Alg_2$ gels, which are then used in a variety of applications for water treatment and as delivery systems. The following section discusses alginate as an adsorbent for water treatment.

## 1.3 Applications of calcium alginate (Ca-$Alg_2$) ionotropic gels

### 1.3.1 Ca-$Alg_2$ as an adsorbent in water treatment

Heavy metal pollution has received considerable attention due to its high toxicity, even at very low concentrations [27]. With the rapid development of industries such as mining operations, metal plating facilities, paper industries and batteries, the

presence of heavy metals in aquatic environments has become one of the most serious environmental concerns [28]. Several methods have been suggested, and applied, for removing heavy metals from aqueous solutions, such as chemical precipitation [29], ion exchange [30], membrane filtration [31], coagulation and flocculation [32], flotation [33], and electrochemical treatment [34]. However, these methods are expensive and can cause serious secondary pollution [28]. On the other hand, adsorption methods have been extensively used due to its simple, relatively low cost and efficiency in removing heavy metal ions from aqueous solutions [35-37].

Alginate materials have been widely used for water treatment applications due to its ability to form stable " egg-box " structures [1], as well as their biocompatibility which means alginate materials are being biologically compatible by not producing a toxic, injurious, or immunologic response in living tissue. Alginate materials are relatively low-cost compared to other polymeric materials [38]. Many studies have shown that the porous structure of ionotropic metal alginates plays a key role in the adsorption of toxic heavy metals from wastewater. For example, Papageorgiou et al. [39] have investigated the ability of calcium alginate (Ca-$Alg_2$) to adsorb $Cu^{2+}$ ions from aqueous solutions [39]. They found that the maximum adsorption capacity of $Cu^{2+}$ ions was 88.95 mg $g^{-1}$, due to the high M-block/G-block ratio. In order to enhance the absorption capacity of Ca-$Alg_2$ recent studies have employed various host materials, such as chitosan [27], magnetic sorbents [40] and kaolin [41]. In particular, alginate–chitosan hybrid gel beads were prepared by Gotoh et al. [27] for the removal of $Cu^{2+}$ ions from wastewater. The adsorption of $Cu^{2+}$ ions on the beads was rapid and reached equilibrium within 10 min with a maximum adsorption capacity of 70 mg $g^{-1}$ [27]. Higher $Cu^{2+}$ ion absorption capacities have been reported using Ca-$Alg_2$ encapsulated with magnetic sorbents (60.0 mg $g^{-1}$ within 3 h) [40] and with Ca-$Alg_2$/kaolin composites (53.6 mg $g^{-1}$ within 2 h) [41].

More recently, the allotropes of carbon such as carbon nanotubes (CNTs) and graphene oxide (GO) have become promising adsorbent materials in the application of water treatment for toxic metal ion removal. For instance, Ca-$Alg_2$/CNTs composites have been shown to have a high $Cu^{2+}$ ion adsorption capacity of 84.9 mg $g^{-1}$ [42]. While GO has been shown to have an excellent $Cu^{2+}$ ion adsorption capacity of 46.6 mg $g^{-1}$ [43].

Part one of this thesis focuses on using Ca-$Alg_2$/GO composite gels for water treatment applications and GO is discussed in detail in the following section.

### 1.3.2 Background on graphene

Carbon forms many allotropes including diamond, graphite (3-dimension (3D)) which is obtained by stacking a large number of graphene sheets (2-dimension (2D)), carbon nanotubes (1-dimension (1D)) which are effectively rolled up sheets of graphene and fullerenes (0-dimension (0D)) which are obtained by wrapping up of graphene sheets, as shown in Figure 1.8 [44].

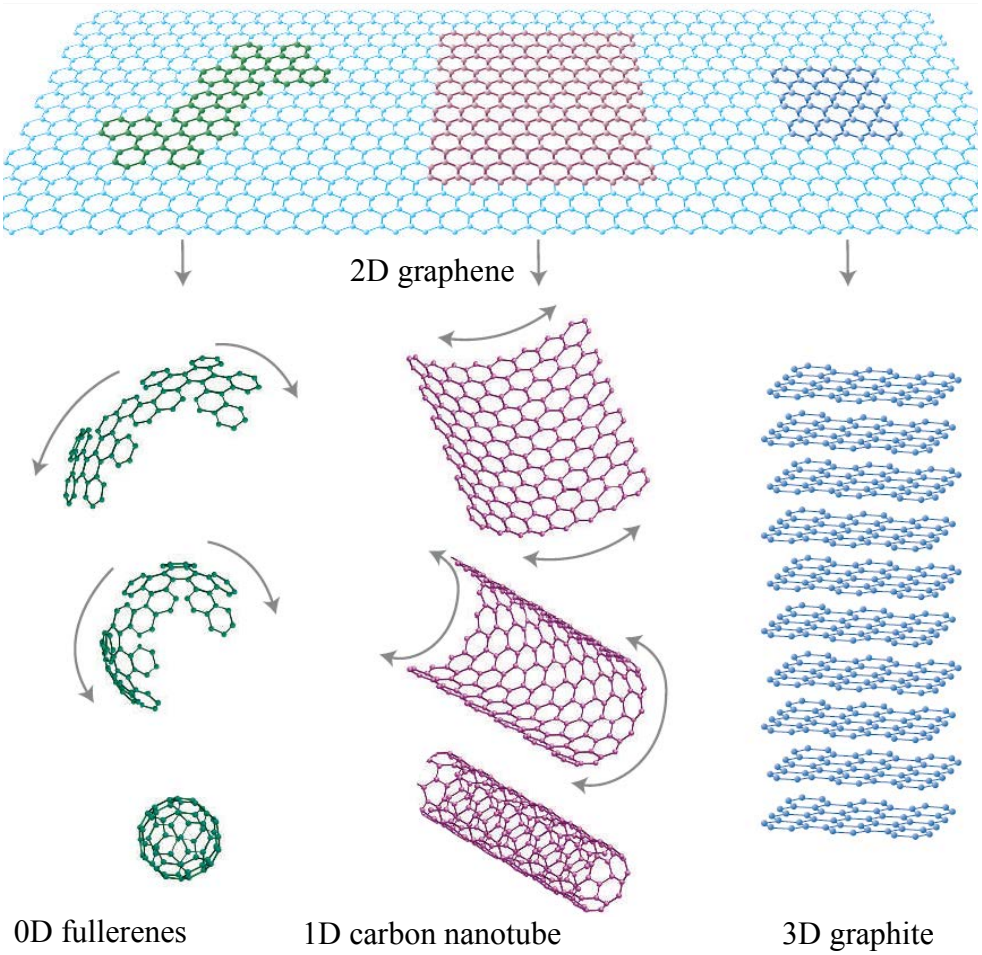


Figure 1-8 Structures of the different allotropes of carbon [44].

Graphene is composed of carbon in a 2D honeycomb lattice [44], with $sp^2$-bonding [45]. It is the main structural element of graphite, which consists of many graphene layers connected together via van der Waals forces. Graphene is very important for many fundamental studies as well as high electron mobility applications such as solar cells, sensors and transparent conductive films because it have high thermal conductivity, high specific surface area and it is the strongest materials [46, 47]. Graphene can be dispersed in water and /or most organic solvents. Recently, many researchers focus on graphite oxide and graphene oxide in their studies [47].

### 1.3.3 Graphite oxide and Graphene oxide (GO)

Graphite oxide, which is a layered material is strongly hydrophilic due to the presence of many functional groups such as hydroxyl, carboxyl and epoxide groups both above and below the basal planes of the sheets, as well as along the edges these functional groups make graphite oxide disperse in water [48]. Graphite oxide is composed of graphene oxide sheets and the interlayer space between the graphene oxide sheets increases from 6 to 12 Å with increasing humidity level [49].

The graphene oxide (GO) structure is described by a single layer with a random distribution of oxidised areas bearing oxygenated functional groups in the form of carboxyl, hydroxyl or epoxy groups wherein the most of the carbon atoms maintain $sp^2$ hybridisation, as shown in Figure 1.9 [50-52]. It should be noted the general structure of GO has yet to be fully elucidated. The average surface roughness is approximately 0.6 nm and the structure is predominantly amorphous due to distortions from $sp^3$ C-O bonds [50].

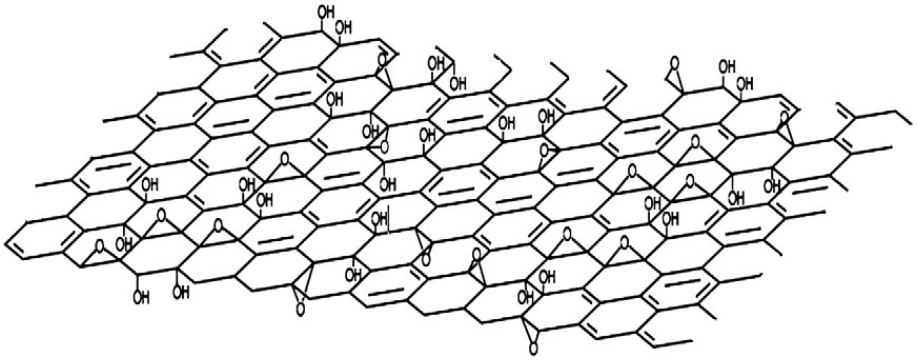

Figure 1-9 A proposed chemical structure of graphene oxide [52].

GO sheets can be easily prepared by full exfoliation of graphite oxide using ultrasonication in water and different organic solvents such as *N*,*N*-dimethylformamide (DMF), *N*-methylpyrrolidone (NMP), tetrahydrofuran (THF) and ethylene glycol [53].

### 1.3.4 Applications of GO

Owing to the extraordinary properties of GO such as high electron mobility, high chemical stability, superior mechanical strength, flexibility and dispersibility in water [54], it has great potential for many applications for example, drug delivery, electronic devices and water treatment, amongst others.

The work on this thesis focuses on applications of GO/Alginate composites for water treatment and as such the following section will highlight recent literature that uses GO for the removal of different pollutants from water.

An important advantage of GO is its very high surface area up to 2620 $m^2$ $g^{-1}$ (theoretical value), and due to this property, GO is a suitable adsorbent for the removal of pollutants in water [55, 56]. For example, the adsorption of $Zn^{2+}$ on GO has been investigated by Wang et al. [56]. The adsorption studies showed that the maximum adsorption capacity was up to 246 mg $g^{-1}$ [56]. The removal of methylene blue from aqueous solution using GO has been studied by Yang et al. [57]. They showed that GO acts as an effective adsorbent material with a high adsorption capacity 714 mg $g^{-1}$ [57].

The widespread use of pharmaceutical antibiotics has become a serious problem for aquatic environments due to their toxicity [58]. For instance, GO was used as an adsorbent for tetracycline removal from aqueous solution by Gao et al. [58]. They found that the maximum adsorption capacity was 313 mg $g^{-1}$ [58]. Chen et al. [59] studied the removal of sulfamethoxazole and ciprofloxacin from aqueous solutions using GO. They demonstrated that GO was an effective adsorbent with high adsorption capacity for the removal of sulfamethoxazole and ciprofloxacin at 379 mg $g^{-1}$and 240 mg $g^{-1}$, respectively [59].

GO composites have also been used for water treatment; for example, GO functionalised magnetic particles (GO-MPs) have been prepared by Lin et al. [60], and utilised as adsorbents for removing tetracycline from aqueous solutions. They observed that the adsorption process was fast and highly efficient with maximum adsorption capacity at 39 mg $g^{-1}$ [60]. Liu et al. [55] have prepared chitosan/graphene oxide (CS/GO) composites for the adsorption of $Au^{3+}$ and $Pd^{2+}$ ions from aqueous solution. The adsorption studies revealed that the maximum adsorption capacity was 1076.6 mg $g^{-1}$ for $Au^{3+}$ and 216.9 mg $g^{-1}$ for $Pd^{2+}$ ions [55]. Fan et al. [61] improved upon the chitosan/graphene oxide (CS/GO) composites by fabricating magnetic chitosan/graphene oxide (MC/GO) nanocomposites, and utilised them for removing $Pb^{2+}$ ions from aqueous solutions. They showed that the maximum adsorption capacity was 76 mg $g^{-1}$ [61].

To understand the adsorption technique the following sections highlights how this method is traditionally carried out and the equations employed to calculate maximum adsorption capacities, which will be used in this thesis.

### 1.3.5 Adsorption technique

Adsorption is a surface process which is commonly expressed as the uptake of an adsorbate by an adsorbent surface [62]. The adsorption equilibrium state is defined by the changeable adsorbed amount (adsorbent loading), adsorbate concentration and temperature [62]. The equilibrium relationship is expressed by Equation 1.2 [62].

$$q_{eq} = f(C_{eq}, T)$$

Equation 1.2

Where $q_{eq}$ is the adsorbed amount at equilibrium, $C_{eq}$ is the adsorbate concentration at equilibrium, and $T$ is the temperature [62].

At constant temperature, the equilibrium relationship can be represented by Equation 1.3 and the adsorption isotherm, see Figure 1.10. Adsorption properties and equilibrium data, commonly known as adsorption isotherms, describe how adsorbates interact with adsorbent materials [63].

$$q_{eq} = f(C_{eq}) \qquad T = \text{constant}$$

Equation 1.3

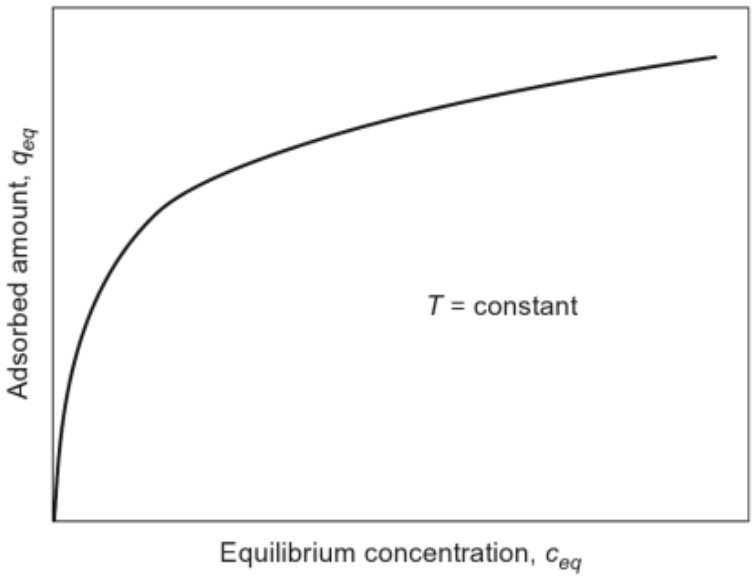


Figure 1-10 Adsorption isotherm [62].

The dependence of the adsorbed amount on the equilibrium concentration is determined experimentally at constant temperature using the bottle–point method

which is usually applied to determine the equilibrium data [62]. In this method each bottle is filled with the adsorbate solution of known volume, $V_L$, and known initial concentration, $C_o$. After adding a defined adsorbent mass, $m_A$, the solution is stirred until a state of equilibrium is reached, see Figure 1.11 [62]. After equilibrium is established, the equilibrium concentration, $C_{eq}$, is measured. Then the adsorbed amount, $q_{eq}$, can be calculated [62].

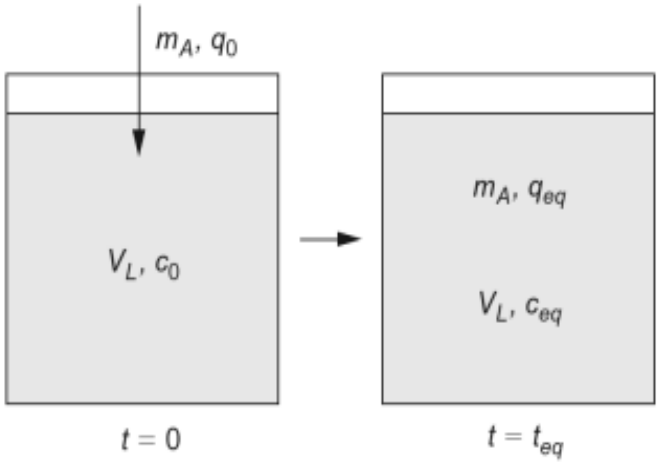


Figure 1-11 Determination of equilibrium data [62].

The mass removed from the liquid phase, $\Delta\, m^l$, must be the same as the mass adsorbed onto the adsorbent, $\Delta\, m^a$, as shown in Equation 1.4 [62].

$$\Delta\, m^l = \Delta\, m^a$$

Equation 1.4

Or as follows Equation 1.5.

$$m_o^l - m_{eq}^l = m_{eq}^a - m_o^a$$

Equation 1.5

The mass concentration, $C$, and the adsorbent loading, $q$, can be simply defined by Equation 1.6 and 1.7, respectively [62].

$$C = \frac{m^l}{V_L}$$

Equation 1.6

$$q = \frac{m^a}{m_A}$$

Equation 1.7

Then Equation 1.4 can be written in the form of Equation 1.8.

$$V_L \left( C_O - C_{eq} \right) = m_A \left( q_{eq} - q_O \right)$$

Equation 1.8

Given that $q_O = 0$ in the equilibrium measurements, Equation 1.8 can be then be reduced to Equation 1.9 [62].

$$q_{eq} = \frac{V_L}{m_A} \left( C_O - C_{eq} \right)$$

Equation 1.9

As the mass in Equation 1.9 is not only valid for the equilibrium state but for each time step of the process, Equation 1.9 can then be written as the general formula described by Equation 1.10

$$q = \frac{V_L}{m_A} \left( C_O - C \right)$$

Equation 1.10

Where $C$ and $q$ are the concentration and the adsorbent loading at a given time, respectively [62].

The most commonly used isotherm equation was proposed by Langmuir (1918) [62], and is as follows:

$$q = \frac{q_m \ b\ C}{1 + b\ C}$$

Equation 1.11

Where $q_m$ and $b$ are the isotherm parameters [62].

In this thesis Equation 1.11 was used to calculate the maximum adsorption capacity for Ca-$Alg_2$ and Ca-$Alg_2$/GO gel beads (refer to Chapter 3, Section 3.5.2 for more details).

The second part of the thesis undertakes research into the use of Ca-$Alg_2$ gels as a delivery system for a variety of dyes and drugs. The following section will highlight background on drug delivery systems related to alginate.

## 1.4 Drug delivery systems

Drug delivery systems can be classified according to the mechanism that controls the release of the drug such as, diffusion controlled systems [64], chemically controlled systems [65], physically activated systems [66], and modulated release systems [67]. The ideal drug delivery system should be biocompatible, mechanically strong and capable of achieving high drug loading [68].

The most important criteria for an effective drug delivery system is that it provides slow release of the drug to the body at a constant rate over a prolonged period of time [69]. Several steps must occur when the drug delivery system is in contact with the

blood stream [70]. The first important step is that the drug must be released from the delivery system; it must then diffuse from the surface of the system to the surrounding blood stream, and it must be transported to its target [70]. Because the release of the drug is totally dependent on the drug delivery system, it should provide a uniform drug concentration as a function of time, require fewer and smaller drug dosages and cause fewer side effects [70].

In the traditional drug delivery systems, the drug level in the blood rises after each administration of the drug and then decreases until the next administration, as shown in Figure 1.12(a) [68, 71]. The most important key with traditional drug delivery systems is that the blood level should remain between a maximum value, which represents a toxic level and a minimum value, which is when the drug is ineffective [68]. The early efforts to prolong drug release involved the use of slowly dissolving coatings and complexes of drugs with suspensions or emulsions [70]. These systems were considered sustained release formulations and provided prolonged drug release over time[70]. However, these systems did not permit long-term release greater than one day [70].

More recent efforts have focused on the use of polymers in the design of a controlled drug delivery systems [70]. In controlled drug delivery systems, the drug level in the blood is prolonged and remains above the minimum value and below the maximum value, as shown in Figure 1.12(b) [68, 71]. The advantages of controlled drug delivery systems are reduction in frequency of the drug administration, reduction in drug fluctuation in the blood and reduction in drug toxicity [68].

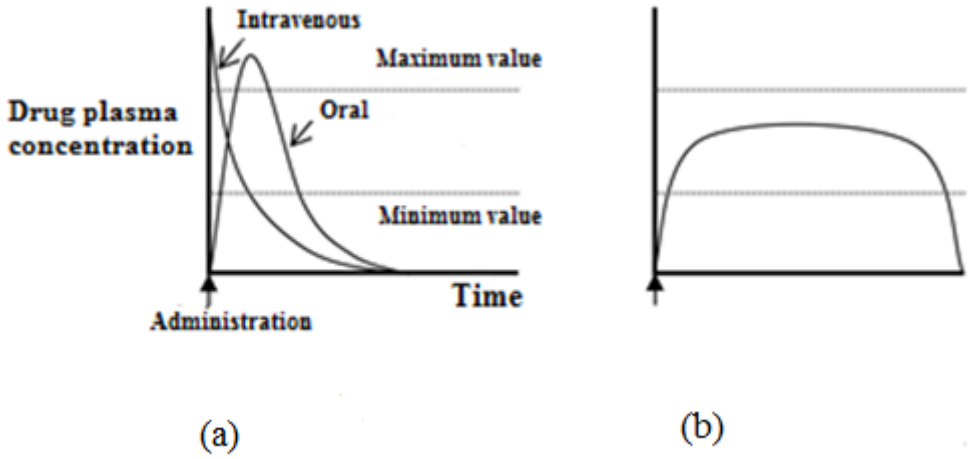


Figure 1-12 Drug release profile (a) traditional drug delivery systems and (b) controlled release systems [71].

Nanoparticles of natural or synthetic polymers, have become an important area in controlled drug delivery system because they have an ability to deliver a wide range of drugs for sustained periods of time to a variety of areas within the body [72]. In particular, chitosan nanoparticles were prepared by spontaneous emulsification [72]. The drug, tacrine, was then released from nanoparticles and was shown to be released in a sustained manner over a period of 12 hours from the chitosan nanoparticles [72]. Shi et al. [73] prepared hydrophobically modified biomineralised polysaccharide alginate membranes via an *in-situ* biomineralisation procedure, as shown in Figure 1.13 [73]. They studied the release of indomethacin from these membranes and found that 60 % of the indomethacin was released within 12 h [73].

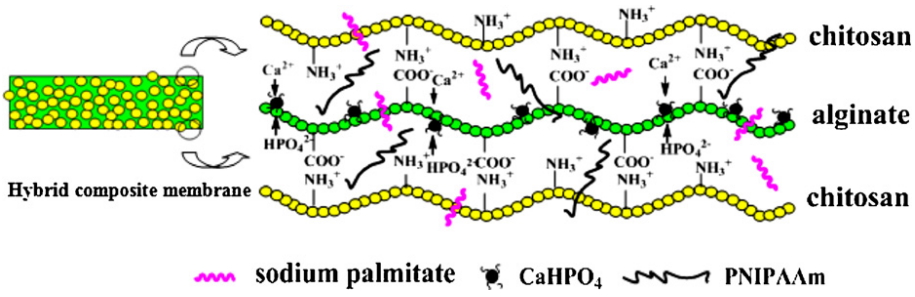


Figure 1-13 Schematic illustration of hydrophobically modified biomineralised polysaccharide alginate membrane [73]

The following section discusses utilising Ca-$Alg_2$ hydrogels as a drug delivery system.

## 1.4.1 Drug delivery systems based on hydrogels

### 1.4.1.1 Hydrogels

Hydrogels are 3D hydrophilic polymeric networks and are able to absorb large quantities of water [74]. Hydrogels of natural polymers such as cellulose, chitosan, starch, dextrin and alginate have attracted much research interest due to their unique advantages, for example, nontoxicity, biocompatibility, and biodegradability [75]. Interestingly, hydrogels can swell to an equilibrium state, and due to this property have been widely used in various biomedical applications for example drug delivery, tissue engineering and wound dressing [76].

Hydrogels can be classified into two categories based on the physical or chemical nature of the cross-linked network [77]. The cross-linked network in a physical hydrogel are held by non-covalent bonds such as hydrogen bonds, hydrophobic interactions and ionic bonds, while in chemical hydrogels the cross-linked network is held together by covalent bonds [77]. They are also classified according to the network electrical charge for example, as cationic hydrogels (chitosan hydrogel) [78], neutral hydrogels (agarose) [79] and anionic hydrogels (Ca-$Alg_2$) [80]. In this work we will employ the anionic hydrogel Ca-$Alg_2$.

Recently, much attention has been focused on utilising polysaccharide hydrogels in biomedical application due to their ability to form a hydrogel. For example, Liu et al. [81] studied the release of camptothecin (CPT) from agar hydrogels using steady-state fluorescence measurements. They also investigated the release kinetics of CPT at different temperatures [81]. They found that the agar hydrogel is a suitable system for the slow release of CPT [81]. Camptothecin is a particularly important drug extracted from the Chinese tree *camptotheca acuminate* and discovered in the early of 1950s by Wall et al. [82]. It has shown significant antitumor activity against a variety of tumours such as lung, ovarian, breast, pancreas and stomach [82, 83]. CPT exists in two forms, the ring–closed lactone form (active against cancer) and the ring–

open carboxylate form (inactive against cancer), as shown in Figure 1.14 [84, 85]. Under neutral and basic pH conditions, the lactone form transforms to the carboxylate form which is not only inactive but also toxic [84]. In attempts to circumvent these problems, significant effort has been made in the synthesis of several drug carriers of CPT by encapsulation into a delivery system. For example, camptothecin has been incorporated into polymeric micelles [86-88], liposomes [89], drug polymer conjugation [90] and microspheres [91, 92]. In this thesis we investigate the encapsulation of CPT into Ca-$Alg_2$ anionic hydrogels.

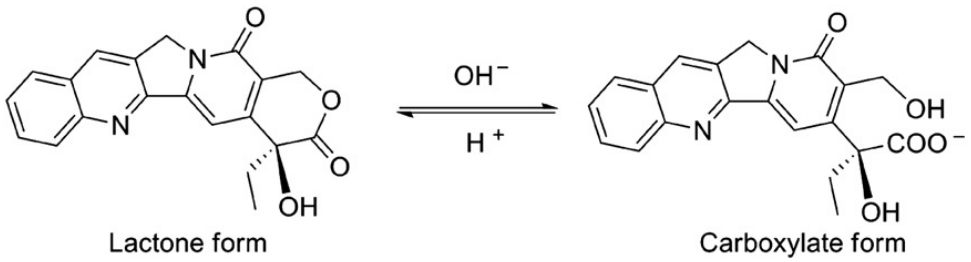


Figure 1-14 Chemical structure of camptothecin and equilibrium reaction between the active lactone form and the inactive carboxylate form [85].

Agarose-κ-carrageenans hydrogel were also prepared by Liu et al. [93]. They studied the release of CPT from these hydrogels after solubilisation of CPT in a cationic surfactant, dodecyltrimethylammonium bromide (DTAB) [93]. They observed that the hydrogel-surfactant systems sustained the release of CPT from the hydrogel [93].

There have been several studies of using alginates in drug delivery systems [94, 95]. The major limiting factor of using Ca-$Alg_2$ hydrogels in drug delivery system is the rapid dissolution of Ca-$Alg_2$ hydrogels at high pH as it results in very fast release of the drug [96]. At high pH the carboxylic acid groups of Ca-$Alg_2$ tends to ionise to give $–COO^-$ groups, which facilitate the swelling of Ca-$Alg_2$ hydrogels. The osmotic pressure inside the Ca-$Alg_2$ hydrogels increases due to the higher concentration of free $H^+$ ions and promote water absorption [97]. To overcome this limitation, many researchers have been focused on blending Na-Alg with another natural polymers

prior to cross-linking [96]. For example, the release of diclofenac from composite beads of Na-Alg and methoxylated pectin cross-linked with $Ca^{2+}$ ions was studied by Pillay and Fassihi [98]. They found that diclofenac released in a sustained manner over a 10 h period from Ca-$Alg_2$-pectinate beads [98]. George and Abraham [96] studied the release of bovine serum albumin (BSA) from sodium alginate–guargum hydrogels cross-linked with glutaraldehyde . It was observed that the release of BSA from this hydrogel increased with increasing pH of the release medium [96]. Dai et al. [99] reported on the preparation of alginate-chitosan mixed beads (Na-Alg solution mixed with chitosan solution prior to cross-linked with $CaCl_2$) and alginate-chitosan coated beads (Ca-$Alg_2$ was first prepared then immersed in chitosan solution) . They investigated the release of nifedipine from these beads [99]. They observed that the amount of nifedipine released from the alginate-chitosan mixed beads was 42 %, whereas this value decreased to 18 % for the alginate-chitosan coated beads at pH ~ 1.5 [99]. They found that the coated beads hold the nifedipine better than the mixed beads at low pH [99]. Nochos et al. [100] investigated the release of BSA from sodium alginate/hydroxypropyl-methylcellulose (Na-Alg/HPMC) beads cross-linked with $Ca^{2+}$ ions. They showed that the addition of HPMC increased the release of BSA from these beads [100].

Colinet et al. [101] reported on the preparation of sodium alginate/poly(ε-caprolactone) cross-linked with $Ca^{2+}$ ions (Na-Alg-g-PCL/ $Ca^{2+}$) beads to study the release of theophylline. They found that the release of theophylline from Na-Alg-g-PCL/ $Ca^{2+}$ beads decreased in low pH solution [101]. They revealed that these beads were able to protect theophylline from acidic solution [101]. Angadi et al. [102] prepared composite blend microbeads consisting of Na-Alg and sodium carboxymethyl cellulose (NaCMC) containing magnesium aluminum silicate (MAS) particles that were coated with chitosan and cross-linked with $Ca^{2+}$ ions. These microbeads were used for controlled release of amoxicillin in a stomach environment [102]. It was observed that the average size of the beads was between 745 and 889 μm [102]. They revealed that these microbeads controlled the release of amoxicillin for up to 8 h at pH ~ 1.2 [102]. The grafting of acrylamide onto hydroxyethyl cellulose (AAM-g-HES) was blended with Na-Alg to prepare microspheres (MPs) by an emulsion-crosslinking method using glutaraldehyde as a crosslinking agent, prepared by AL-Kahtani and Sherigara [103]. The release of diclofenac from MPs

was studied and they observed that the release of diclofenac increased with an increasing ratio of AAM-g-HES in the beads [103].

Drug delivery systems face a major problem with poor water solubility of many useful drugs. The following section focuses on how β-cyclodextrin can be used improve drug solubility and thus improve drug delivery systems.

### 1.4.2 Cyclodextrins (CDs) for improved drug delivery systems

Some drugs in the pharmaceutical industries are significantly restricted by their poor solubility in aqueous media and highly toxic side effects [104]. In order to overcome the solubility of these drugs an inclusion complex between the hydrophobic drug and cyclodextrins (CDs) has been shown to be a worthwhile strategy [105]. CDs, discovered in 1891, are cyclic oligosaccharides made up of six (α-cyclodextrin), seven (β-cyclodextrin) or eight (γ-cyclodextrin) glucopyranose monomers connected via α–(1-4) bonds, thus creating a truncated cone shape as shown in Figure 1.15 [106, 107]. The structure of CDs comprises of primary hydroxyl groups ($C_6$) at the narrow edge of the cone and secondary hydroxyl groups ($C_2$ and $C_3$) at the wider edge, resulting in a hydrophilic outer surface as shown in Figure 1.15 [106]. The central cavity is structurally composed of skeletal carbons and ethereal oxygen groups, which give it a lipophilic environment, as shown in Figure 1.15 [106, 107].

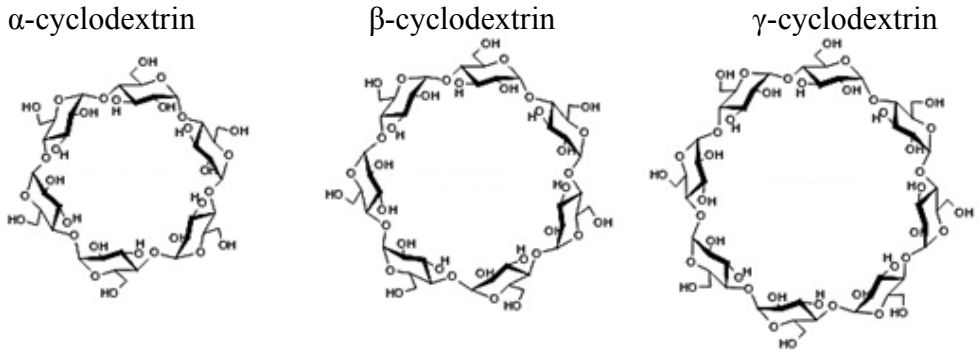


Figure 1-15 Structure of cyclodextrins [107].

A special characteristic of CDs is their ability to form inclusion complexes (host-guest complexes) with various guest molecules, as shown in Figure 1.16 [108, 109] In these complexes, the guest molecules is held within the cavity by non-covalent bonds [108]. Host-guest complexes enhance the properties of the guest molecules for example the solubility and the stability [108]. Additionally, CD provides a controlled and sustained release of drugs in the drug delivery system [106]. β-CD is widely used because of its low cost and its larger internal cavity diameter (narrow rim is ~6.4 Å and the wide rim is ~15.4 Å) is suitable for a wide range of guest molecules [108].

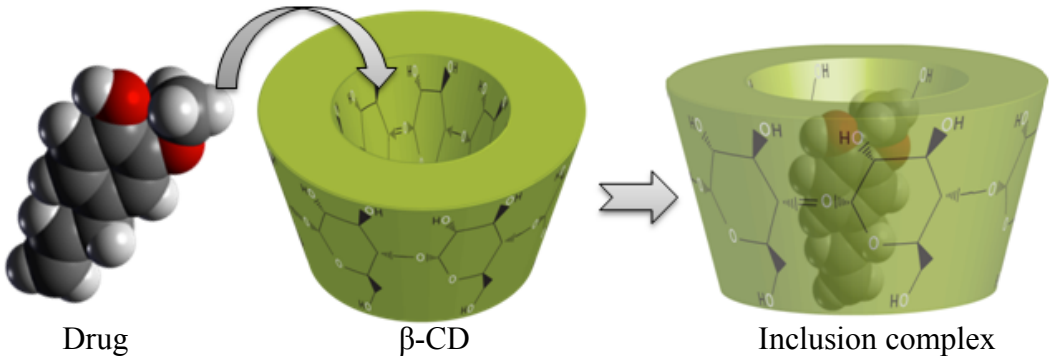


Figure 1-16 Structure of the inclusion complex [109].

Sambasevam et al. [110] synthesised an inclusion complex between the poorly water soluble drug azomethine and β-CD. They characterised the complex using Fourier transform infrared (FTIR) spectroscopy, $^{1}$H nuclear magnetic resonance ($^{1}$H NMR) spectroscopy and thermogravimetric analysis (TGA) and showed that an inclusion complex formed where the benzyl part of azomethine was included into the hydrophobic cavity of the β-CD [110]. A dibenzalacetone (DBA) and β-CD inclusion complex (β-CD/DBA) was prepared by Periasamy et al. [111]. They confirmed the interaction between β-CD and DBA by FTIR spectroscopy, X-ray diffraction (XRD), differential scanning calorimetry (DSC) and microscopic morphological image analysis [111]. They showed that the 1:1 stoichiometry of the β-CD/DBA inclusion complex was the most highly probable model, as shown in Figure 1.17 [111].

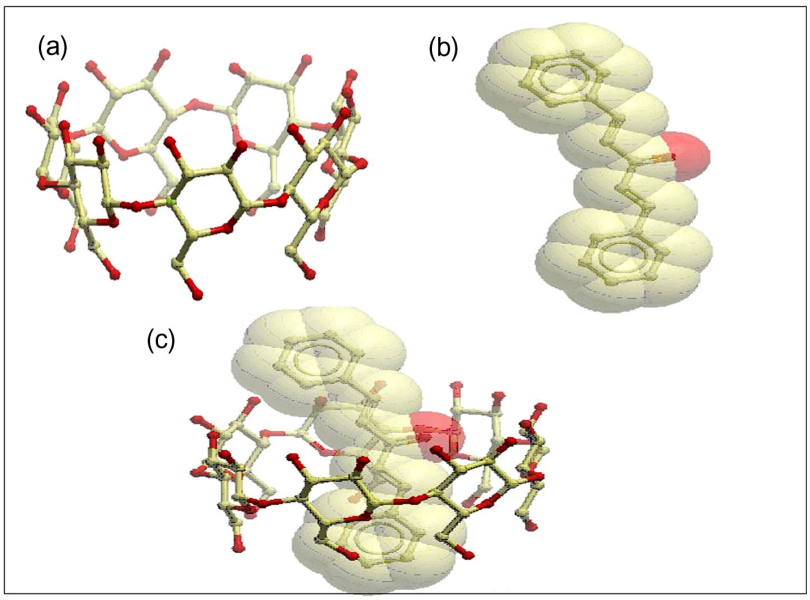


Figure 1-17 3D structural representation of (a) β-CD, (b) DBA and (c) β-CD/DBA inclusion complex [111].

Wang et al. [112] synthesised an inclusion complex between soybean lecithin and β-CD (β-CD/soybean lecithin). Soybean lecithin is easy to oxidise and sensitive to heat and light, which restricts its pharmaceutical application [112]. They characterised the complex using FTIR, DSC and XRD and showed that an inclusion complex formed [112]. They found that the molar ratio of β-CD/soybean lecithin was 2:1, and they revealed that the thermal stability of soybean lecithin in the inclusion complex was significantly improved compared with free soybean lecithin [112]. Chen et al. [113] prepared crassicauline A (CLA) with β-CD (β-CD/CLA), and characterised using FTIR, DSC and XRD. They revealed that the molar ratio of β-CD/CLA was 1:1, as shown in Figure 1.18 [113]. They found that the water solubility and thermal stability of CLA were increased in the inclusion complex [113].

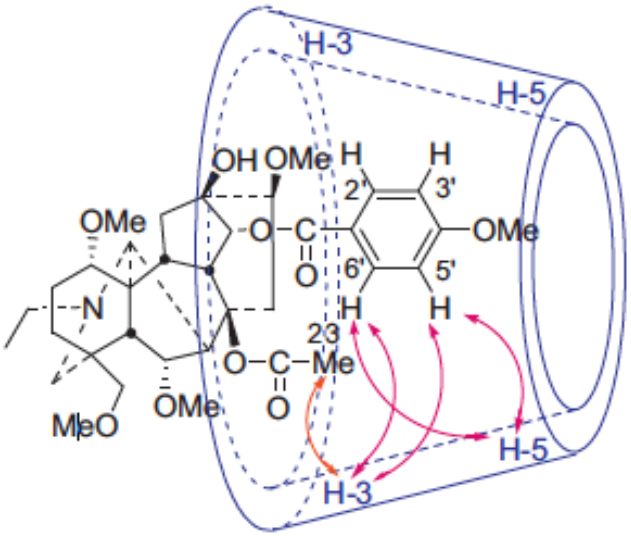


Figure 1-18 Possible β-CD/CLA inclusion complex mode [113].

The inclusion complex of garlic acid with β-CD (β-CD/garlic acid) was prepared by Wang et al. [114], and the release of garlic acid from the inclusion complex was studied. FTIR, DSC and XRD analysis confirmed the preparation of the inclusion complex, and they found that the molar ratio of β-CD/garlic oil was 1:1 [114]. The release of garlic acid from the inclusion complex was determined at a temperature range from 25 to 50 °C, and they found that at room temperature the inclusion complex was very stable and no garlic oil was released from the inclusion complex [114]. However, the garlic oil release from the inclusion complex increased with increasing temperature [114]. They revealed that β-CD protected the garlic oil against evaporation after it was included in the cavity of the β-CD [114]. They further investigated the release of the garlic oil from the inclusion complex in acidic medium (pH ~ 1.5) at 37 °C, and they found that after 12 h that the garlic oil was completely release from the inclusion complex [114].

Given the poor water solubility of CPT and its toxic side- effects, Kang et al. [115] have investigated the effects of cyclodextrins such as α-CD, β-CD, (γ-CD, hydroxypropyl-β-cyclodextrin (HP-β-CD), randomly substituted dimethyl-β-cyclodextrin (RDM-β-CD) and randomly substituted dimethyl-γ-cyclodextrin (RDM-γ-CD) on the solubility, stability, and cytotoxicity of CPT. They found that cyclodextrins were effective complexing agents and could be used to improve the

solubility and stability of CPT [115]. They observed that there was an increase in the activity of CPT in the presence of cyclodextrins rather than free CPT, for example, HP-β-CD/CPT and RDM-β-CD/CPT was more active than free CPT in concentrations from $1.0 \times 10^{-6}$ to $1.0 \times 10^{-7}$ M and from $1.0 \times 10^{-6}$ to $1.0 \times 10^{-9}$ M, respectively. They attributed the improved stability of CPT in the complexes was due to the CPT being less prone to hydrolysis than free CPT [115].

Studies have focused on designing novel drug delivery systems which conjugate β-CD units with polymers to enhance drug stability [116]. When a great number of β-CD units are congregated on a polymer, the formation of numerous hydrogen bonds between β-CD and the polymer leads to a more compact polymer coil [117]. Hollas et al. [117] investigated the complexation of pyrene into the cavity of pure β-CD and β-CD substituted poly(allylamine). They found that the complexation ratio between β-CD and pyrene was 1:1 and 2:1 inclusion complexes, as shown in Figure 1.19(a) [117]. They revealed that β-CD polymer exhibited a significant change in the complexation behaviour depending on the degree of substitution [117]. They revealed that if the degree of substitution below 5 %, 1:1 inclusion complexes dominated rather than 1:2 inclusion complexes, due to a hindered intramolecular formation of 2:1 inclusion complexes [117]. Due to long distances between adjacent β-CD units and a high loss in the entropy of the polymers, the 2:1 inclusion complexes were unfavourable as shown in Figure 1.19(b) [117]. If the degree of substitution was up to 23 %, intermolecular 2:1 inclusion complexes from neighbouring polymer chains were more favourable. The reason for this behaviour is due to the smaller distance between adjacent β-CD units [117].

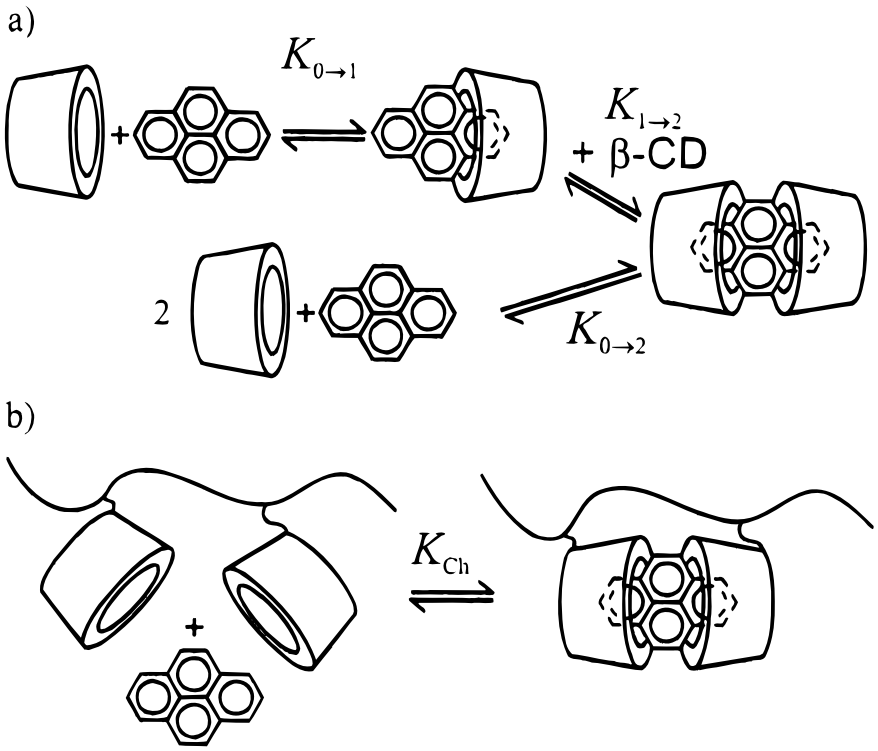


Figure 1-19 Schematic representation of the 2:1 inclusion complexes (a) 2:1 inclusion complexes from pure β-CD and (b) 2:1 inclusion complexes from β-CD polymer [117].

### 1.4.3 β-cyclodextrin grafted polymers as drug delivery system

Hollow nanospheres based on β-cyclodextrin-grafted-α, β-poly (aspartic acid) (β-CD-*graft*-PAsp) have been developed as a drug carrier for CPT by Zeng et al. [116]. The synthesis details are shown in Figure 1.20. Stability, cytotoxicity and CPT release were studied. They observed that the active lactone form of CPT was protected from hydrolysis under physiological conditions [116]. They found that the CPT/β-CD-*graft*-PAsp exhibited sustained release of CPT up to 10 days while the free CPT was released completely during 24 h. Furthermore, they revealed that the CPT/β-CD-*graft*-PAsp showed less toxicity after 48 h exposure than free CPT, and resulted in the slow release of CPT from the CPT/β-CD-*graft*-PAsp [116].

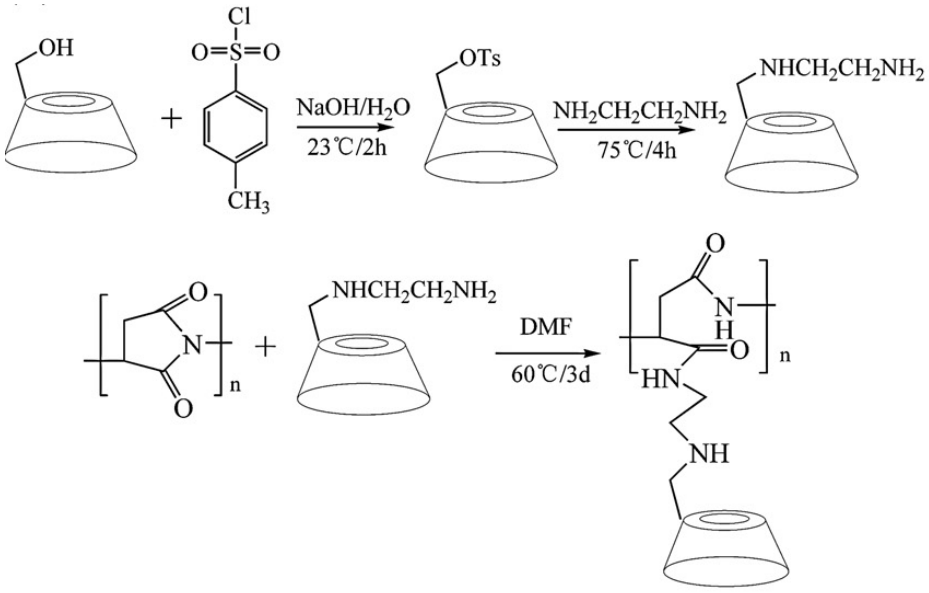


Figure 1-20 Synthesis scheme of β-CD-*graft*-PAsp [116].

More recently, Du et al. [104] have prepared a polymer nanoparticle delivery system (average size 98 nm) based on a β-cyclodextrin-grafted diblock copolymer poly(ethylene glycol) and poly(L-glutamic acid) with CPT, synthesis details are shown in Figure 1.21.

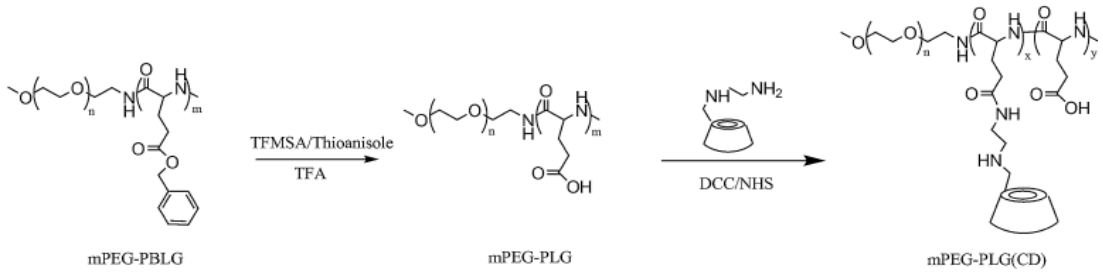


Figure 1-21 Synthesis scheme of mPEG-PLG(CD) [104]

They studied the stability, cytotoxicity and CPT released from the polymer nanoparticles and observed that the polymer nanoparticles enhanced the stability of the CPT against hydrolysis under physiological condition [104]. They found that the polymer nanoparticles exhibited a sustained release of CPT over 6 days while the free CPT was released completely within 24 h. Furthermore, they revealed that the polymer nanoparticles were less cytotoxic than free CPT due to the gradual CPT release from the nanoparticles [104].

## 1.5 Summary

Na-Alg polymer has been used widely for water treatment applications. The gelling of Na-Alg (e.g. Ca-$Alg_2$) is mainly achieved in the presence of divalent or trivalent cations with a specific structure (egg-box). The porous structure of ionotropic metal alginates plays an important role in the adsorption of heavy metal from wastewater. Recent studies have employed Na-Alg with host materials even with nanotubes to enhance their adsorption capacity.

Na-Alg is an excellent candidate for drug delivery due to its unique properties, such as biocompatibility, biodegradability and non-toxicity. However, the rapid dissolution of Ca-$Alg_2$ hydrogels at high pH is the major limiting factor, as it results in very fast release of the drug. To overcome this limitation, many researchers have focused on blending Na-Alg with another natural polymers prior to cross-linking.

Some of the drugs in the controlled drug delivery systems are significantly restricted by their poor solubility in aqueous media and highly toxic side effects. Recent advances offer numerous controlled drug delivery systems based on using cyclodextrins (CDs) especially β-CD, due to their ability to form inclusion complexes with a wide range of guest molecules. To enhance the stability of the hydrophobic drug, many researcher conjugate β-CD units with polymers.